

Baroclinic Instabilities of the Two-Layer Quasigeostrophic Alpha Model

DARRYL D. HOLM

*Theoretical Division and Center for Nonlinear Studies, Los Alamos National Laboratory, Los Alamos, New Mexico, and
Mathematics Department, Imperial College of Science, Technology and Medicine, London, United Kingdom*

BETH A. WINGATE

*Computer and Computational Science Division and Center for Nonlinear Studies, Los Alamos National Laboratory,
Los Alamos, New Mexico*

(Manuscript received 18 June 2004, in final form 26 November 2004)

ABSTRACT

The class of alpha models for turbulence may be derived by applying Lagrangian averaging to the exact fluid equations and then making a closure approximation based on Taylor's hypothesis of frozen-in fluctuations. This derivation provides a closed expression for the unknown pseudomomentum in the generalized Lagrangian mean theory of Andrews and McIntyre. In the current study, the mean effects of turbulence on baroclinic instability are explored, as determined by the two-layer quasigeostrophic-alpha model in quasigeostrophic (QG) balance. The QG-alpha model is found to lower the critical wavenumber, reduce the bandwidth of instability, and preserve the value of forcing at onset in the baroclinic case. It also preserves the fundamental dependence of baroclinic instability on the gradient of the potential vorticity. These results encourage using the alpha-model approach—based on combining Lagrangian averaging with Taylor's hypothesis closure approximations—in simulations of global ocean circulation, because this class of turbulence closure models allows Lagrangian-averaged effects of baroclinic instability to be simulated on a coarse mesh.

1. Introduction

Baroclinic instability converts available potential energy to kinetic energy. This instability is fundamental to understanding energy and mass transport in fluid dynamics. Coarse-resolution global ocean models often cannot resolve the Rossby deformation radius, the length scale required to predict baroclinic instability. As a consequence, some subgrid models attempt to mimic baroclinic instability on coarse computational meshes.

This work shows how a Lagrangian-averaged turbulence model affects the onset of baroclinic instability and quasigeostrophic (QG) shear instability. Lagrangian averaging produces the modification to the nonlinearity in the Navier–Stokes equations introduced

by Holm et al. (1998). The length scale α is the average correlation length associated with the covariance tensor $\overline{\xi\xi}$ for the fluctuating displacement $\xi(x, t) = x(x_0, t) - \bar{x}(x_0, t)$ of a Lagrangian fluid parcel trajectory away from its Lagrangian mean trajectory with the same fluid label x_0 . In practice, the correlation length α represents the smallest active scale in the solution, below which the dynamics at smaller scales may be regarded as passively transported. Thus, the smaller scales are not diffused, as in Eulerian averaging. Instead, they are “dragged,” or “swept” by the fluid motion of the larger scales.

With the choice of viscous dissipation introduced in Chen et al. (1998), the Lagrangian-averaged Navier–Stokes alpha (LANS-alpha) equations preserve basic fluid properties while regularizing the Navier–Stokes equations. In specific terms, the LANS-alpha equations preserve Kelvin's circulation theorem and their energy dissipation controls the H^1 norm of the fluid velocity. Moreover, the LANS-alpha regularization of the Navier–Stokes equations is accomplished through

Corresponding author address: Beth Wingate, Los Alamos National Laboratory, MS B284, Los Alamos, NM 87545.
E-mail: wingate@lanl.gov

modifying the nonlinearity of fluid dynamics, not through added dissipation. As a consequence, Foias et al. (2001) proved existence and uniqueness of global strong solutions for the LANS-alpha equations in periodic domains. They also showed that these solutions converge to solutions of Navier–Stokes as $\alpha \rightarrow 0$ and that such solutions have a finite-dimensional global attractor. These results are not available for the Navier–Stokes equations, which are recovered upon setting $\alpha \rightarrow 0$ in the LANS-alpha equations. Of further interest, the LANS-alpha equations may be interpreted as a turbulence closure for the generalized Lagrangian mean (GLM) equations of Andrews and McIntyre (1978). In this closure, the pseudomomentum of GLM theory is modeled as being proportional to the curvature of the velocity flow lines. Papers discussing other results of the LANS-alpha equations can be found in Chen et al. (1998, 1999a,b), Nadiga and Margolin (2001), Holm and Nadiga (2003), Nadiga and Shkoller (2001), B. A. Wingate (2005, unpublished manuscript), Geurts and Holm (2002, 2003), and Fabijonas and Holm (2003).

This work investigates, using standard mathematical techniques, the effects of accounting for the effects of the small scales on the large scales through Lagrangian averaging on baroclinic stability and compares the results with those from an Eulerian-averaging-style eddy viscosity model. To illustrate the effects of the Lagrangian model, consider the Eady problem as discussed in Pedlosky (1987, his section 7.7). Pedlosky's Eq. (7.7.4) changes to

$$(z - c) \left\{ \frac{1}{S} \frac{\partial^2}{\partial z^2} \Phi + [1 - \alpha^2(\partial_{yy} - k^2)](\partial_{yy} - k^2)\Phi \right\} = 0,$$

and the boundary conditions are unchanged. Then, the definition of μ , which is representative of the horizontal wavenumber [Pedlosky's Eq. (7.7.9)], is $\mu^2 = (k^2 + l_n^2)[1 + \alpha^2(k^2 + l_n^2)]S$. When $\alpha = 0$, we recover the unaveraged values of μ , but when α is finite it changes μ as a function of horizontal wavenumber. We illustrate this in Fig. 1a.

Figures 1b–d (Pedlosky's Figs. 7.7.1a, 7.7.1b, and 7.7.2a) show the changes to some of Pedlosky's results (see caption for details). The main point is that incorporating the effects of the small scales on the large scales through Lagrangian averaging has the effect of moving the stability to a lower wavenumber and decreasing the growth rates by redefining the potential vorticity. Although the Eady problem is interesting, the gradient of potential vorticity is zero. Therefore the current work investigates the corresponding effects of the α model on the classical, two-layer baroclinic insta-

bility problem for the QG- α model, which has a non-zero PV gradient.

a. Outline

The paper is organized as follows. We begin by introducing the Lagrangian averaging modifications for the QG- α equations in their multilayer representation. The QG- α equations incorporate the circulation effects of frozen-in fluctuations into their definition of potential vorticity (PV). This fundamental change in the PV is a recurring theme in the interpretations of the QG- α model that we discuss for baroclinic instability in the sections that follow.

Section 2 demonstrates the effects of incorporating turbulence in the redefinition of PV as PV- α on the classic two-layer baroclinic instability. We illustrate the effects of QG- α on the two-layer baroclinic instability in the following three cases: no vertical shear; no β effect; and the general case, in which both the vertical shear and the β effect are nonzero. We also discuss the effects of PV- α on the two-layer baroclinic growth rates and neutral curves. We also compare these results with those of a simple eddy viscosity model.

Section 3 presents and discusses the Howard–Miles theorem and linearized stability of QG- α equilibrium solutions. The treatment in section 3 of formal stability of two-layer QG- α equilibria emphasizes the role of PV- α in modeling the QG effects of turbulence. This treatment relies on the Hamiltonian formulation of the inviscid QG- α equations, in which equilibrium solutions appear as critical points of energy, constrained by local conservation of PV- α . The criterion for linearized stability of these QG- α equilibria is obtained from the condition that the second variation of the constrained energy provides a norm for the perturbations, when it is evaluated at the equilibrium. This second variation is preserved by the linearized evolution of the perturbations. As a consequence, imposing the equilibrium conditions that provide a conserved norm also controls the linear growth of the perturbations. Both the sufficient conditions for linearized stability and the converse necessary conditions for instability in the Howard–Miles theorem for QG- α turn out to be expressed in terms of gradient PV- α of the equilibrium solutions. Last, we collect the main results of the paper in a brief summary that emphasizes the role of gradient PV- α as the underlying mechanism for the Lagrangian-averaged QG, two-layer baroclinic instability.

b. Layer model QG- α

The new multilayer QG- α equations with a free surface are given, for the geometry given in Fig. 2, by the local potential vorticity conservation law,

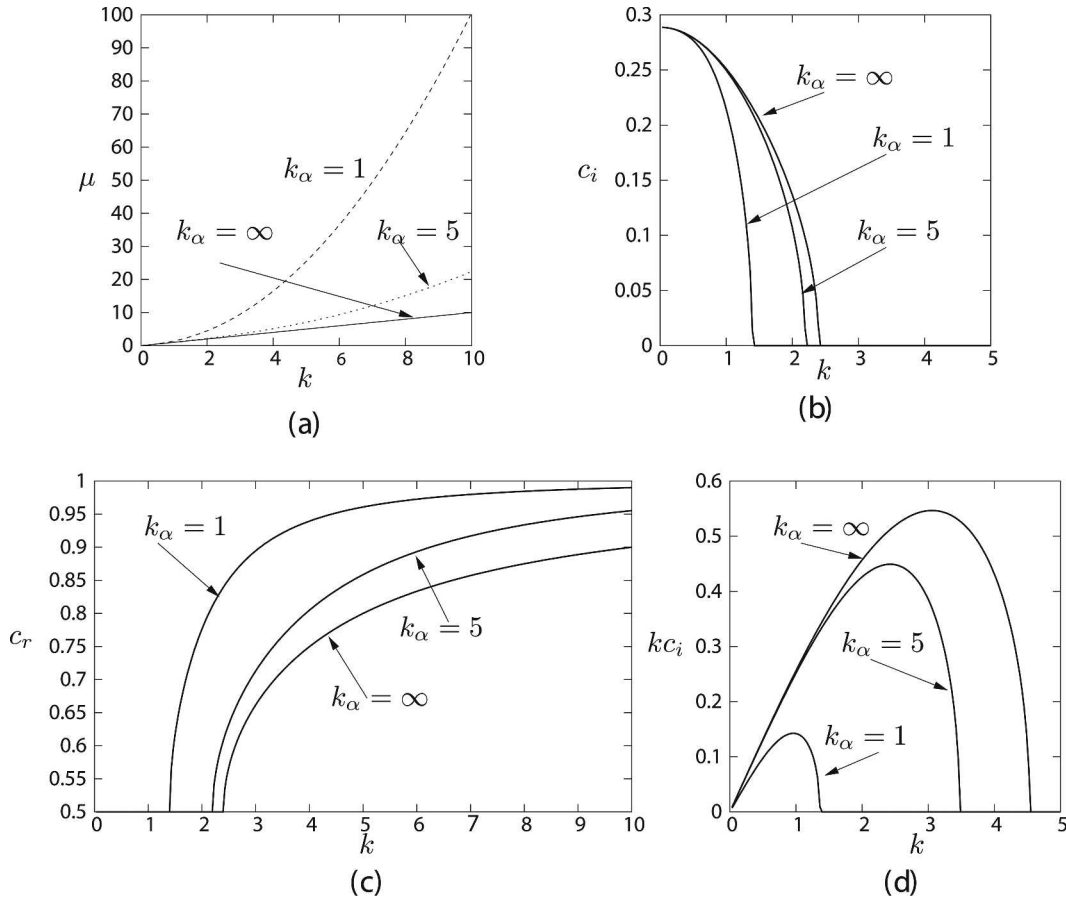


FIG. 1. (a) The linear relationship for $k_\alpha = \infty$ ($\alpha = 0$) between μ and k for the unaveraged case. As we decrease k_α (increase α), we show that for a given k , μ increases quadratically. (b), (c) Pedlosky's Figs. 7.7.1a and 7.7.1b show the changes to the real and imaginary parts of the phase speed. Notice that the coalescence at the critical wavenumber still occurs but that the critical wavenumber is decreased. (d) Pedlosky's Fig. 7.7.2a shows that the growth rates decrease as k_α decreases (α increases).

$$\frac{\partial q_i}{\partial t} + \mathbf{u}_i \cdot \nabla q_i = 0 \quad \text{with} \quad \mathbf{u}_i = \hat{\mathbf{z}} \times \nabla \psi_i. \quad (1)$$

The alpha-modified potential vorticity q_i (PV- α) in the i th layer is defined in terms of the streamfunction ψ_i for each layer,

$$q_i = \nabla^2(1 - \alpha^2 \nabla^2) \psi_i + F_i \sum_{j=1}^N T_{ij} \psi_j + f \quad \text{with} \quad F_i = \frac{f_0^2}{g'H_i^2}. \quad (2)$$

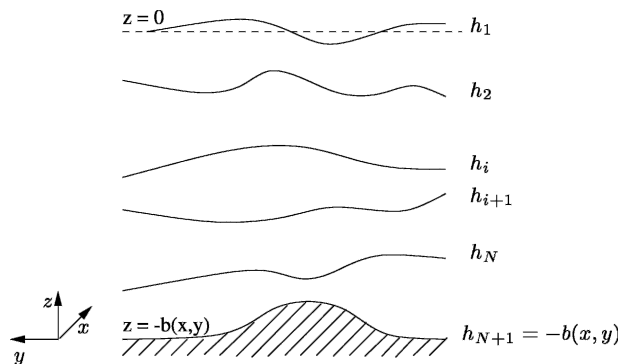


FIG. 2. The geometry for the N -layer model.

Denote \mathbf{T} as the $N \times N$ symmetric tridiagonal second-difference matrix,

$$\mathbf{T} = \begin{bmatrix} -1 & 1 & 0 & \dots & \dots \\ 1 & -2 & 1 & \dots & \dots \\ 0 & 1 & \dots & \dots & \dots \\ \dots & \dots & \dots & -2 & 1 \\ \dots & \dots & \dots & 1 & -1 \end{bmatrix}. \quad (3)$$

The effect of the pseudomomentum closure, based on Taylor's hypothesis of frozen-in fluctuations, results in the alpha-modification of the elliptic operator in the

potential vorticity q_i for the i th layer in Eq. (2). In what follows, we shall use periodic boundary conditions in the horizontal direction. However, for other boundary conditions, when the Helmholtz operator in Eq. (2) for PV- α has a nontrivial kernel, an additional boundary condition will be required in determining the streamfunction from PV- α . Use of period boundary conditions avoids this issue.

2. Baroclinic instability—Two-layer model

The two-layer QG model, first studied by Phillips (1954), is the simplest system that exhibits baroclinic instability. We follow Phillips by specializing the multilayer QG- α equations to two layers and linearizing about a basic state with constant vertical shear. We use

the rigid-lid approximation and set $H_1 = H_2 = H/2$, which imposes $F_1 = -F_2 = F$, where $2F = k_{\text{int}}^2$, and k_{int} is the internal deformation wavenumber. For two layers, Eq. (1) becomes

$$\frac{\partial q_j}{\partial t} + J(\psi_j, q_j) = 0 \quad \text{for } j = 1, 2, \quad (4)$$

with

$$q_1 = \nabla^2(1 - \alpha^2 \nabla^2)\psi_1 + F(\psi_2 - \psi_1) + f \quad \text{and} \quad (5)$$

$$q_2 = \nabla^2(1 - \alpha^2 \nabla^2)\psi_2 + F(\psi_1 - \psi_2) + f, \quad (6)$$

where $F = f_0'(g'H_i) = k_{\text{int}}/2$. One linearizes around the basic state by setting $\psi_1 = -Uy + \psi_1'$ and $\psi_2 = Uy + \psi_2'$, where U is a constant velocity. Substituting in the traveling wave relations, taking the determinant, and solving for the frequency produces the dispersion relation

$$\omega = -\frac{k\beta[k_{\text{int}}^2 + 2k_h^2 A(k_h, \alpha)]}{2k_h^2 A(k_h, \alpha)[k_{\text{int}}^2 + k_h^2 A(k_h, \alpha)]} \pm \frac{k\sqrt{4U^2 k_h^4 A(k_h, \alpha)^2 [k_h^4 A(k_h, \alpha)^2 - k_{\text{int}}^4] + \beta^2 k_{\text{int}}^4}}{2k_h^2 A(k_h, \alpha)[k_{\text{int}}^2 + k_h^2 A(k_h, \alpha)]}, \quad (7)$$

where $A(k_h, \alpha) = (1 + \alpha^2 k_h^2)$. Thus, the standard two-layer dispersion relation for QG changes for QG- α by the substitution $k_h^2 \rightarrow k_h^2 A(k_h, \alpha)$. Instability occurs when the discriminant is negative, which requires

$$\beta^2 k_{\text{int}}^4 < 4U^2 k_h^4 A(k_h, \alpha)^2 [k_{\text{int}}^4 - k_h^4 A(k_h, \alpha)^2]. \quad (8)$$

We illustrate the effects of QG- α on the two-layer baroclinic instability in the following cases: (i) no vertical shear; (ii) no β effect; (iii) the general case, in which both the vertical shear and the β effect are non-zero; (iv) the growth rates; and (v) the comparison with an eddy viscosity model.

a. No vertical shear, $U = 0$

For the case of no vertical shear, one sets $U = 0$ in Eq. (7) and finds, as expected, a slow baroclinic wave and a fast barotropic wave, whose dispersion relations are

$$\text{(baroclinic)} \quad \omega_1 = \frac{-k\beta}{k_h^2 A(k_h, \alpha) + k_{\text{int}}^2} \quad \text{and} \quad (9)$$

$$\text{(barotropic)} \quad \omega_2 = \frac{-k\beta}{k_h^2 A(k_h, \alpha)}. \quad (10)$$

These two dispersion relations are shown in Fig. 3b. The solid lines describe the baroclinic mode for different values of αk_{int} , and the dotted lines describe the barotropic mode. The barotropic frequency diverges to infinity near the origin because the external deformation wavenumber for the rigid-lid formulation is infi-

nite. When $\alpha \rightarrow 0$, the classical result is that both of the waves are stable. Lagrangian averaging preserves this classical result. The model arising from Lagrangian averaging produces results for the two-layer dispersion relation that resemble those for the barotropic QG- α model. In particular, as α increases, the Rossby deformation wavenumber decreases, and ω decreases at high wavenumbers.

b. No beta effect, $\beta = 0$

Next, we consider constant rotation. For the QG case, the long waves are unstable and the short waves are stable. Setting $\beta = 0$ in the dispersion relation in Eq. (7) yields

$$\omega(k) = \pm kU \sqrt{\frac{k_h^2 A(k_h, \alpha) - k_{\text{int}}^2}{k_h^2 A(k_h, \alpha) + k_{\text{int}}^2}}. \quad (11)$$

Thus, instability occurs when

$$f = (k_h/k_{\text{int}})^2 [1 + (\alpha k_{\text{int}})^2 (k_h/k_{\text{int}})^2] - 1 < 0, \quad (12)$$

as depicted in Fig. 3c for $\alpha k_{\text{int}} = 0, 1/2$, and 1. Setting $\alpha = 0$ in Eq. (11) recovers the usual baroclinic stability criterion for $\beta = 0$. Wavenumbers greater than the internal Rossby deformation wavenumber are unstable, and wavenumbers lower than the Rossby deformation wavenumber are stable. Thus, setting $\alpha \neq 0$ in the Lagrangian-averaged two-layer QG- α model shifts the onset of instability toward lower wavenumber.

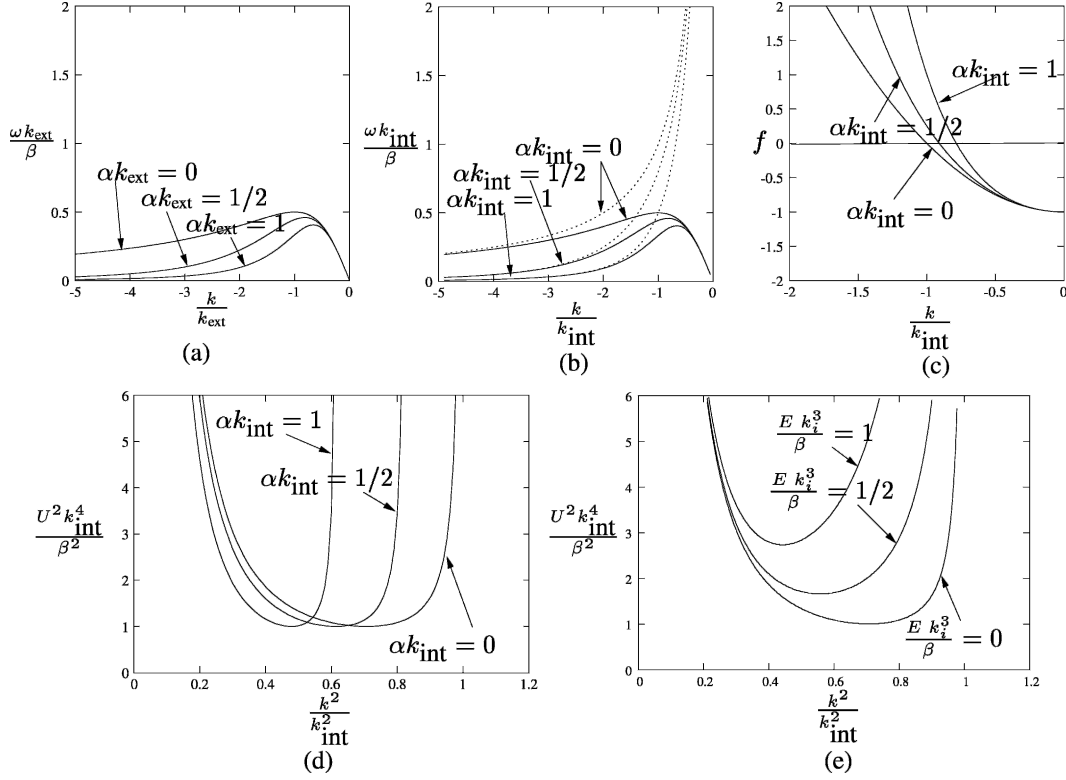


FIG. 3. (a) The dispersion relation for the frequency $\omega(k)$ for the barotropic QG- α equations. The alpha model decreases the Rossby deformation wavenumber k_{ext}^α at which the maximum frequency occurs. It also decreases the frequency for high wavenumbers while closely approximating the frequency at low wavenumbers. (b) For $U = 0$, the Rossby deformation wavenumber (at the peak of the dispersion relation) shifts toward wavenumbers of lower magnitude. The baroclinic waves are represented by solid lines, and the barotropic lines are dotted. The barotropic lines diverge as $k \rightarrow 0$, because of the rigid-lid assumption. (c) For $\beta = 0$ and $l = 0$, the onset of instability occurs when f crosses from negative to positive, where f is the discriminant in Eq. (11) and is defined in Eq. (12). This onset also shifts toward wavenumbers of lower magnitude as αk_{int} increases. (d) The neutral curve for the Lagrangian-averaged model. It shows for $U \neq 0$ and $\beta \neq 0$ that the critical wavenumber at the minimum of the neutral curve also shifts toward lower wavenumber as αk_{int} increases. Note that the onset of instability remains at the same value of forcing, independent of αk_{int} . (e) Changes to the neutral curve for the eddy viscosity model for three different values of Ek_{int}^3/β . We conclude that both the Lagrangian-averaged alpha model and the Eulerian-averaged eddy viscosity model lower the critical wavenumber, but in different ways. The Lagrangian-averaged alpha model uses dispersion, whereas the eddy viscosity model uses damping. Because of this extra dissipation, the eddy viscosity model requires a higher forcing for the onset of baroclinic instability.

c. The neutral curve, $\beta \neq 0$, $U \neq 0$

The neutral curve in Eq. (8) is shown in Fig. 3d. For $\alpha = 0$ this formula recovers the expected result for the classical two-level baroclinic instability problem. The critical wavenumber for the onset of instability in this case is $k_c^2 = (1/\sqrt{2})k_{\text{int}}^2$ and the critical shear is $U^2 = \beta^2/k_{\text{int}}^4$.

For $\alpha \neq 0$, the fundamental stabilizing effect of β is preserved, and the minimum shear needed to produce instability remains unchanged. However, the alpha model lowers the critical wavenumber to

$$k_c^2(\alpha) = \frac{-1 + (1 + 2\sqrt{2}\alpha^2 k_{\text{int}}^2)^{1/2}}{2\alpha^2} \leq \frac{1}{\sqrt{2}} k_{\text{int}}^2. \quad (13)$$

The Lagrangian averaging process also decreases the bandwidth of unstable wavenumbers. The instability bandwidth is limited to $k_h^2 < k_{\text{int}}^2$ for the QG equations, because the neutral curve for two-layer baroclinic instability becomes vertical at wavenumber $k_b^2 = k_{\text{int}}^2$ and higher wavenumbers are stable. For the QG- α model, verticality of the neutral curve occurs at the limiting wavenumber,

$$k_b^2(\alpha) = \frac{-1 + (1 + 4\alpha^2 k_{\text{int}}^2)^{1/2}}{2\alpha^2} \leq k_{\text{int}}^2. \quad (14)$$

Thus, for any forcing, the limiting unstable wavenumber decreases as alpha increases. This effect reduces the bandwidth of unstable waves for QG- α .

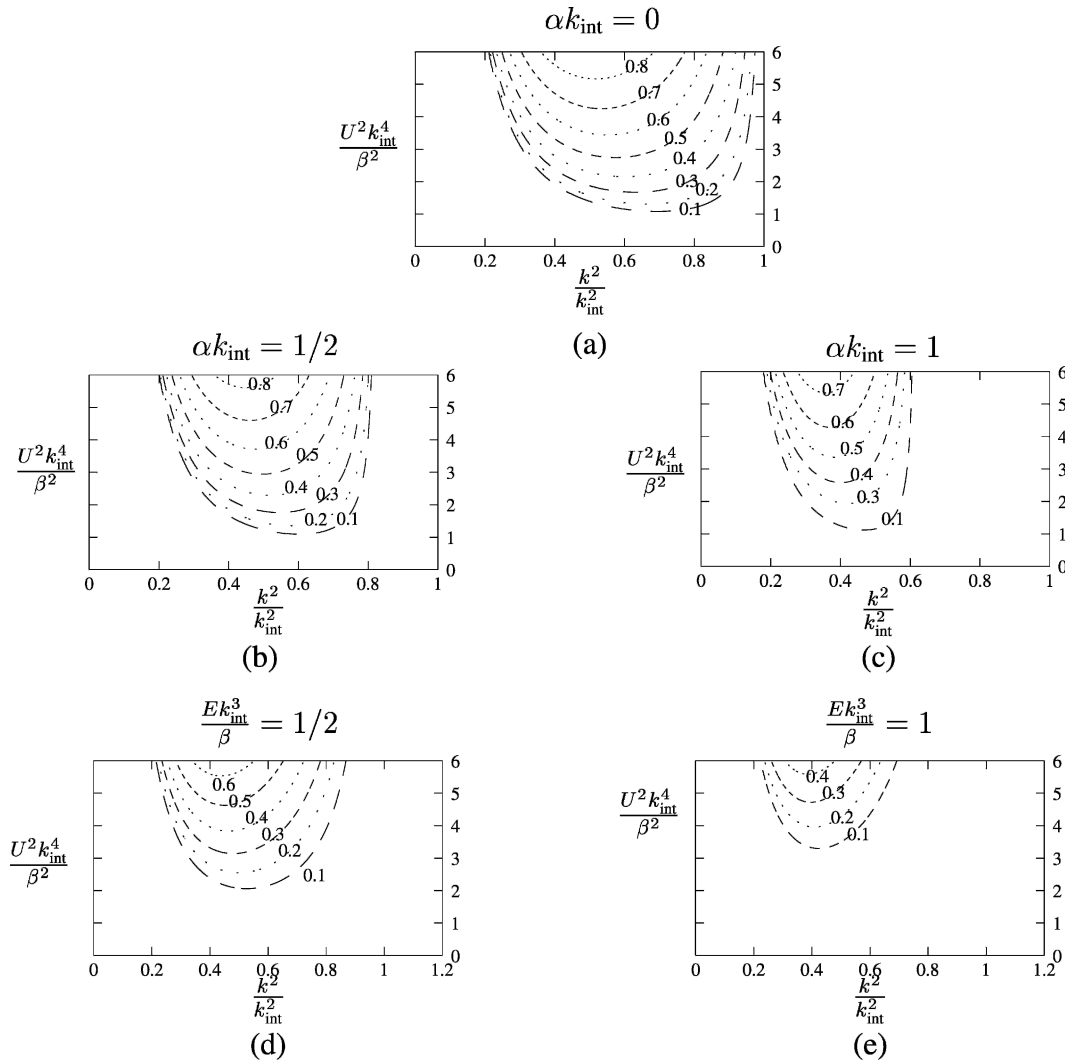


FIG. 4. Growth rates. Two-layer alpha-model growth rates, $\text{Im}(\omega)k_{\text{int}}/\beta$ for the case $\beta \neq 0$, $U \neq 0$, and $l = 0$. The growth rates slightly decrease as αk_{int} increases and the unstable region compresses into a smaller bandwidth. Two-layer eddy viscosity growth rates, $\text{Im}(\omega)k_{\text{int}}/\beta$, for the case $\beta \neq 0$, $U \neq 0$, and $l = 0$. The growth rates decrease and require a higher forcing for the onset of instability.

d. Growth rates

Figure 4 shows the numerically computed, nondimensional growth rates for the case in which $\beta \neq 0$, $U \neq 0$, and $l = 0$. These growth rates are $k_{\text{int}} \text{Im}(\omega)/\beta$, with ω given in Eq. (7). Figure 4a shows the case for no averaging ($\alpha = 0$). As αk_{int} is increased (Figs. 4b,c), the growth rates are compressed into the smaller bandwidth described by the alpha-modified neutral curve. In contrast, Figs. 4d and 4e show the corresponding plots of the growth rates when eddy viscosity is imposed instead of the alpha modifications.

We plot the maximum growth rate against the parameter αk_{int} in Fig. 5a. For three different values of the forcing $U^2 k_{\text{int}}^4/\beta^2$, Fig. 5a shows that the growth rate

decreases as αk_{int} increases. For the highest forcing shown, the decrease in maximum growth rate over the range of values of αk_{int} was about 20%. The location of the maximum growth rate, also computed numerically, is shown in Fig. 5b. For all values of αk_{int} shown, the alpha model lowers the wavenumber of the maximum growth rate.

e. Effects of eddy viscosity

Most Eulerian-averaged turbulence models produce second-order terms that introduce additional dissipation into the partial differential equation. There are several favorite kinds of dissipation for the QG equations that have been investigated analytically for two-

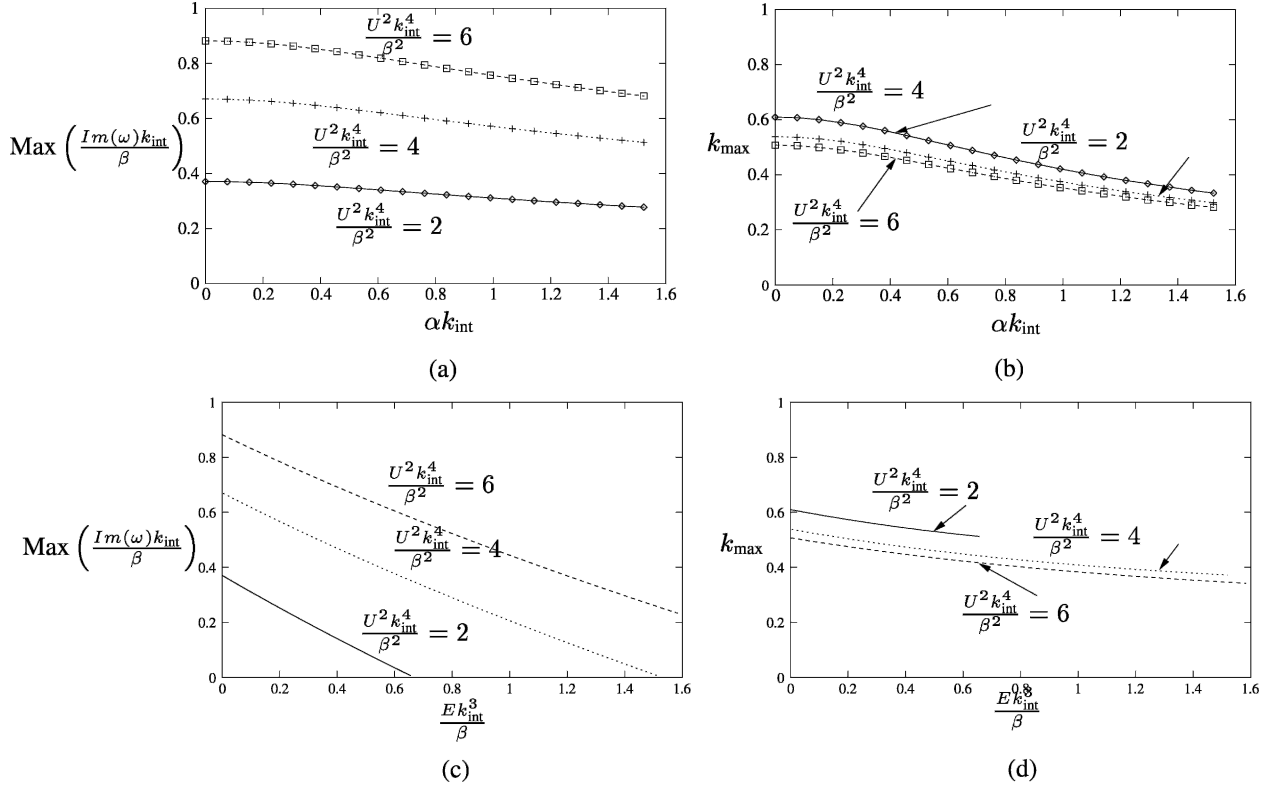


FIG. 5. (a) The maximum growth rate decreases as a function of αk_{int} for three different values of the shear to rotation parameter $U^2 k_{\text{int}}^4/\beta^2$. (b) The wavenumber location of the maximum growth rate is reduced as we increase αk_{int} . We conclude that one effect of the Lagrangian-averaged model is to suppress the growth rates and to lower the wavenumber where the maximum occurs. (c) The maximum growth rate decreases substantially as the viscosity is increased relative to β for three values of the forcing $U^2 k_{\text{int}}^4/\beta^2$. The growth rates go to zero for the two lowest values of the forcing shown, quenching the instability. (d) The location at which this maximum occurs decreases with viscosity. The lines “end” relative to the viscosity because the fluid is no longer unstable (maximum growth rate is zero).

layer model baroclinic instability by Klein and Pedlosky (1992) and numerically by Holland and Haidvogel (1980). It seems unclear whether adding dissipation through eddy viscosity in baroclinically unstable geophysical flows has the desired effect of modeling unresolved eddy activity. For example, Klein and Pedlosky concluded that even qualitative behavior was dependent upon the type and strength of the dissipation, and Holland and Haidvogel found that in their numerical investigation the dissipation had almost no discernible effect for the values of the eddy viscosity that were, at that time, used in numerical ocean models. Thus, the question of whether eddy viscosity provides a proper representation of unresolved eddy activity remains an unsettled issue. We shall not contribute to the resolution of this larger question. Rather, we shall discuss its simplest aspects in the current framework, with the purpose of comparing the two different mechanisms of modeling the effects of the small scales on the large scales, specifically dissipation versus nonlinear transport.

Because our purpose is to juxtapose a Lagrangian-averaged method of incorporating the effects of the small scales on the large scales to that of an Eulerian method, we focus on the simplest eddy viscosity model that dissipates potential vorticity. Hence, the right-hand side of Eq. (4) changes to

$$\frac{\partial q_i}{\partial t} + J(\psi_i, q_i) = Eq_i, \tag{15}$$

with potential vorticity q_i given in Eqs. (5)–(6). We linearize about the basic state, as in section 2. After some algebra, the dispersion relation with eddy viscosity included is

$$\omega(k) = \frac{-\beta k(F + k_h^2) \pm k[U^2 k_h^4(k_h^4 - 4F^2) + F^2 \beta^2]^{1/2}}{k_h^2(2F + k_h^2)} - iEk_h^2. \tag{16}$$

Equation (16) is the same as the classical dispersion relation except for the last term, which represents the

wavenumber-dependent damping expected from eddy viscosity. When ω has a positive imaginary part, the waves grow exponentially and instability occurs. When ω has a negative imaginary part, the amplitude of ψ is damped. Therefore, the last term on the right-hand side of Eq. (16) may cancel contributions to the imaginary part of the equations when the square root is negative, thereby lowering the critical wavenumber.

Figure 3e shows the numerically computed neutral curve for the eddy viscosity model in Eq. (15). As viscosity increases relative to β the critical wavenumber moves to lower wavenumber, similar to the effect of increasing α . The effects of eddy viscosity and the alpha regularization differ in two important ways, however. First, as eddy viscosity increases, the forcing necessary to produce instability also increases. Therefore, baroclinic instability in an eddy viscosity model requires increased forcing. Second, eddy viscosity does not decrease the bandwidth of unstable waves. The neutral curve for eddy viscosity at high forcing asymptotically approaches the inviscid case, and so the unstable bandwidth is not reduced.

Contour plots of the growth rates for baroclinic instability with eddy viscosity are shown in Figs. 4d and 4e, where we see that the neutral curves shift upward to higher forcing, and the growth rates decrease as eddy viscosity is increased.

Now compare Figs. 5a and 5c, which both show the maximum growth rate as a function of the relevant modeling parameter. For the Lagrangian-averaged model this parameter is αk_{int} , and for the eddy viscosity model it is Ek_{int}^3/β . Both models decrease the maximum growth rate, but the eddy viscosity will eventually quench the baroclinic instability entirely. This phenomenon is also apparent in Figs. 5b and 5d. These figures show the wavenumber location of the highest growth rate as a function of the model parameter for three different values of the forcing. Both models lower the wavenumber at which the maximum growth rate occurs for a given forcing. Both models change the baroclinic instability results for some wavenumbers. Eddy viscosity may remove the instability for all wavenumbers, however.

3. Howard–Miles theorem and Arnold’s stability for the two-layer QG- α model

This section presents and discusses the Howard–Miles theorem and formal stability of two-layer QG- α equilibria.

a. Howard–Miles theorem

Pedlosky (1963) generalized the Howard–Miles theorem Howard (1961); Miles (1961) for the incompressible

stratified 2D Euler equations to the case of the two-layer QG model. In this case, one begins from a different basic state than was used earlier for the classical two-layer problem. Substitute $\psi_1 = -\Psi_1(y) + \psi'_1$ and $\psi_2 = -\Psi_2(y) + \psi'_2$ into Eqs. (4)–(5), linearize, and then Fourier transform in x . After some manipulation, we integrate between two points y_1 and y_2 in the spanwise direction and apply the boundary conditions, $p_1 = p_2 = dp_1/dy = dp_2/dy = 0$ at $y = y_1$ and $y = y_2$, to arrive at the analog for the QG- α model of Pedlosky’s Eq. (2.3) for QG:

$$2ic_i \int_{y_0}^{y_1} dy \left(\frac{|p_1|^2}{|\Psi_{1y} - c|^2} \frac{\partial q_1}{\partial y} + \frac{|p_2|^2}{|\Psi_{2y} - c|^2} \frac{\partial q_2}{\partial y} \right) = 0. \quad (17)$$

From this formula one may draw the same Howard–Miles conclusion for the QG- α model as Pedlosky did for the QG equations: For instability $c_i \neq 0$, and so the potential vorticity gradients must be positive in some regions and negative in others. The same is true for PV- α gradients in the QG- α model. By its original derivation from the Euler–Poincaré theory, the QG- α model preserves the structure of the QG equations. As we shall discuss in the next section, this structure is closely associated with the Hamiltonian formulations of both sets of equations. However, the QG- α model changes the definition of PV to PV- α , as in Eq. (5).

b. Formal stability of two-layer QG-alpha equilibria

An equilibrium solution of a dynamical system is formally stable, if a conserved quantity is found whose first variation vanishes at the solution and whose second variation evaluated at the equilibrium solution is positive (or negative) definite. In this case, the second variation provides a conserved norm for the dynamics of the linearized equations, which implies linearized stability. By linearized stability, we mean that evolution under the linearized equations stays within a neighborhood of the equilibrium, defined by the norm of the initial displacement. This behavior, in turn, implies spectral stability, because it forbids exponential growth.

Following Holm et al. (1985, 32–35), one may analyze the formal stability and convexity analysis for nonlinear stability of two-layer QG-alpha equilibria by using the energy-Casimir method of Holm et al. (1985). The results follow the same energy-Casimir procedure as for standard multilevel QG in Holm et al. (1985), modulo changing the elliptic operators in the definitions of PV- α as q_j in Eqs. (2), (5), and (6) to include composition of the Helmholtz operator $(1 - \alpha^2 \nabla^2)$ with the

Laplacian (∇^2) in those definitions. In particular, the Lie–Poisson Hamiltonian formulation, Casimir conservation laws, interpretation of equilibria as constrained critical points of the sum of the energy and conserved Casimirs, linearized Lyapunov (formal) stability conditions obtained from the second variation of this sum, and finally the a priori estimates needed for proving convexity and thus establishing nonlinear Lyapunov stability of these equilibrium solutions all follow from the standard energy-Casimir method established in Holm et al. (1985).

PHYSICAL INTERPRETATION OF THE FORMAL STABILITY CONDITIONS

In physical terms, the results from the energy-Casimir stability method state the following sufficient condition for a steady QG- α flow to be stable: when straddling the streamlines of such a flow, the q -vorticity of the equilibrium flow increases to the right. In particular, consider a steady shear QG- α flow that satisfies this stability condition with $u_i^e(y) \hat{x}$ and choose a Galilean frame in which the velocity $u_i^e(y)$ has a single sign. In such a flow, a sufficient condition for stability is that the quantity $\partial_y q_i^e$ (grad PV- α) does not change sign. Thus, the sufficient condition for stability (that grad PV- α not change sign) is the *converse* of the necessary condition for *instability* implied by the Howard–Miles theorem for the quadratic form in Eq. (17). In the latter case, for instability to occur, grad PV- α must have different signs in different regions of the flow.

As a consequence, the sufficient condition for formal stability and the necessary condition for instability in the Howard–Miles theorem for equilibrium solutions of QG- α are consistent with each other, because they are both expressed in terms of the same fundamental quantity, grad PV- α . When $\alpha \rightarrow 0$, the corresponding results are recovered for the QG model.

4. Summary

Grad PV is the underlying mechanism of baroclinic instabilities. Lagrangian averaging preserves this instability mechanism. Our analysis shows how the alpha model based on Lagrangian averaging preserves the role of grad PV in the explicit formulas for stability and instability. For two-layer baroclinic instability, the effect of Lagrangian averaging was to lower the critical wavenumber and narrow the bandwidth of unstable waves. The QG- α equations preserved the fundamental stability criterion in terms of grad PV while redefining PV as PV- α .

To elucidate the difference between Lagrangian av-

eraging and eddy viscosity for the baroclinic instability problem, we showed that the eddy viscosity model also lowers the critical wavenumber. However, because it dissipates both energy and PV gradient, models with eddy viscosity require a higher forcing for the onset of baroclinic instability. It was also clear from the linear stability analysis that eddy viscosity moves the onset of instability to lower wavenumber through amplitude damping, whereas the Lagrangian-averaged alpha-model uses dispersion.

The results, especially for baroclinic instability, suggest the use of alpha models in global ocean simulations because, by solving for the Lagrangian-averaged fields, the decrease in the Rossby deformation wavenumber makes baroclinic instability resolvable on a coarse mesh. The alpha model's narrowing of the bandwidth of unstable waves also has a numerical advantage in that the higher wavenumbers are prevented from generating high-frequency noise in the solution.

Acknowledgments. We are grateful to the Turbulence Working Group at Los Alamos for many constructive discussions and thoughtful remarks. We are also grateful to R. C. Malone for his encouragement and helpful suggestions. One of us (DDH) was partially supported during the course of this work by the U.S. DOE Office of Scientific Computing.

REFERENCES

- Andrews, D. G., and M. E. McIntyre, 1978: An exact theory of nonlinear waves on a Lagrangian-mean flow. *J. Fluid Mech.*, **89**, 609–646.
- Chen, S. Y., C. Foias, D. D. Holm, E. J. Olson, E. S. Titi, and S. Wynne, 1998: The Camassa–Holm equations as a closure model for turbulent channel and pipe flows. *Phys. Rev. Lett.*, **81**, 5338–5341.
- , —, —, —, —, and —, 1999a: The Camassa–Holm equations and turbulence in pipes and channels. *Physica D*, **133**, 49–65.
- , —, —, —, —, and —, 1999b: A connection between the Camassa–Holm equations and turbulence in pipes and channels. *Phys. Fluids*, **11**, 2343–2353.
- Fabijonas, B. R., and D. D. Holm, 2003: Mean effects of turbulence on elliptic instability in fluids. *Phys. Rev. Lett.*, **90**, doi:10.1103/PhysRevLett.90.124501.
- Foias, C., D. D. Holm, and E. S. Titi, 2001: The Navier–Stokes-alpha model of fluid turbulence. *Physica D*, **152–153**, 505–519.
- Geurts, B. J., and D. D. Holm, 2002: Leray simulation of turbulent shear layers. *Advances in Turbulence IX: Proceedings of the Ninth European Turbulence Conference*, I. P. Castro and P. E. Hancock, Eds., CIMNE, Barcelona, Spain, 337–340.
- , and —, 2003: Regularization modeling for large-eddy simulation. *Phys. Fluids*, **15**, L13–L16.
- Holland, W. R., and D. B. Haidvogel, 1980: A parametric study of the mixed instability of idealized ocean currents. *Dyn. Atmos. Oceans*, **4**, 185–215.
- Holm, D. D., and B. T. Nadiga, 2003: Modeling mesoscale turbu-

- lence in the barotropic double-gyre circulation. *J. Phys. Oceanogr.*, **33**, 2355–2365.
- , J. E. Marsden, T. Ratiu, and A. Weinstein, 1985: Nonlinear stability of fluid and plasma equilibria. *Physics Rep.*, **123**, 1–116.
- , —, and —, 1998: Euler-Poincaré models of ideal fluids with nonlinear dispersion. *Phys. Rev. Lett.*, **80**, 4173–4177.
- Howard, L. N., 1961: Note on a paper of John W. Miles. *J. Fluid Mech.*, **10**, 509–512.
- Klein, P., and J. Pedlosky, 1992: The role of dissipation mechanisms in the nonlinear dynamics of unstable baroclinic waves. *J. Atmos. Sci.*, **49**, 29–48.
- Miles, J. W., 1961: On the stability of heterogeneous shear flow. *J. Fluid Mech.*, **10**, 496–508.
- Nadiga, B. T., and L. G. Margolin, 2001: Dispersive–dissipative eddy parameterization in a barotropic model. *J. Phys. Oceanogr.*, **31**, 2525–2531.
- , and S. Shkoller, 2001: Enhancement of the inverse-cascade of energy in the two-dimensional Lagrangian-averaged Navier–Stokes equations. *Phys. Fluids*, **13**, 1528–1531.
- Pedlosky, J., 1963: Baroclinic instability in two layer systems. *Tellus*, **15**, 20–25.
- , 1987: *Geophysical Fluid Dynamics*. 2d ed. Springer-Verlag, 710 pp.
- Phillips, N. A., 1954: Energy transformations and meridional circulations associated with simple baroclinic waves in a two-level, quasi-geostrophic model. *Tellus*, **6**, 273–286.